AGU PUBLICATIONS

JGR

Journal of Geophysical Research: Biogeosciences

RESEARCH ARTICLE
10.1002/2016JG003491

Special Section:
The Arctic: An AGU Joint Special Collection

Key Points:
- Tundra groundwater is an important source of methane to areas of the lake where the water to air dissolved methane flux is also higher
- Isotope analyses suggest that bacteria methyl-type fermentation is the major pathway of methane production in the active layer
- Changes in precipitation in the Arctic could induce changes in methane production in groundwater due to changes in saturated zone thickness

Supporting Information:
- Supporting Information S1

Correspondence to:
A. L. Lecher,
alecher@lynn.edu

Citation:
Lecher, A. L., P.-C. Chuang, M. Singleton, and A. Paytan (2017), Sources of methane to an Arctic lake in Alaska: An isotopic investigation, *J. Geophys. Res. Biogeosci.*, *122*, 753–766, doi:10.1002/2016JG003491.

Received 18 MAY 2016
Accepted 10 MAR 2017
Accepted article online 15 MAR 2017
Published online 11 APR 2017

©2017. American Geophysical Union. All Rights Reserved.

Sources of methane to an Arctic lake in Alaska: An isotopic investigation

Alanna L. Lecher[1,2], Pei-Chuan Chuang[1], Michael Singleton[3], and Adina Paytan[4]

[1]Earth and Planetary Sciences, University of California, Santa Cruz, California, USA, [2]Natural and Applied Sciences, Lynn University, Boca Raton, Florida, USA, [3]Nuclear and Chemical Sciences Division, Lawrence Livermore National Laboratory, Livermore, California, USA, [4]Institute of Marine Sciences, University of California, Santa Cruz, California, USA

Abstract Sources of dissolved methane (CH_4) at Toolik Lake, Alaska, include both diffusion from lake sediments and groundwater entering the lake from its perimeter. Here we use hydrogen and oxygen isotopes in water (H_2O), carbon and hydrogen isotopes in CH_4, and carbon isotopes in dissolved inorganic carbon (DIC) to calculate the relative importance of lake sediment and groundwater discharge as sources of dissolved CH_4 to Toolik Lake. We also resolve the relative importance of the source contribution spatially within the lake and determine the processes controlling CH_4 concentrations in groundwater surrounding the lake. Our findings, from a mixing model based on isotopes in CH_4, suggest that groundwater is a more important source of CH_4 at the perimeter of the lake where the water-to-air flux is high. Additionally, we find on the local scale that high groundwater methane concentrations may be better linked to areas around the lake where rain is the dominant source of water to the active layer, indicating that changes in precipitation and active layer thaw depth will impact methane concentrations in the active layer and, ultimately, the groundwater associated flux to Toolik Lake.

Plain Language Summary This project investigates the cycling of methane, a green house gas, at an Arctic Lake in Alaska. The study shows that increases in rain could cause an increase in the amount of methane transported to Arctic lakes.

1. Introduction

Methane (CH_4) is an important greenhouse gas in the Earth's atmosphere with a greenhouse forcing 25 times higher than carbon dioxide (CO_2) on time scales less than 100 years [*Badr et al.*, 1991]. Atmospheric CH_4 has increased from 1600 ppb to about 1800 ppb in the last decade [*Dlugokencky et al.*, 2009]. Global warming is expected to enhance CH_4 release into the atmosphere and result in a positive feedback effect [*Anisimov*, 2007]. In terms of the global atmospheric CH_4 budget, total CH_4 emission to the atmosphere is on the order of 500–600 Tg CH_4 yr^{-1}, and the largest portion of natural sources (23%) is released from wetlands including those from high latitudes [*Reeburgh*, 2013]. It has been suggested that some fraction of the observed increase in CH_4 attributed to wetland sources is related to permafrost thawing [*Anisimov*, 2007]. An estimated mass of 9.5×10^5 Tg C is contained in Northern Hemisphere permafrost, and Arctic lakes are estimated to presently emit more than 20 Tg of CH_4 $year^{-1}$ globally [*Walter et al.*, 2007; *Zimov et al.*, 2006].

Studies have shown that groundwater discharge can transport CH_4 to Toolik Lake from the Arctic tundra [*Paytan et al.*, 2015], to the Arctic and North Pacific Ocean [*Lecher et al.*, 2015], and to the Gulf of Mexico [*Bugna et al.*, 1996]. Groundwater discharge at Toolik Lake predominately enters the lake from the lake perimeter, which is also the area of highest water to air diffusive CH_4 flux [*Dimova et al.*, 2015; *Garcia-Tigreros Kodovska et al.*, 2016; *Paytan et al.*, 2015]. It was inferred from limited δ^{13}C-CH_4 isotope data that the source of CH_4 to groundwater surrounding Toolik Lake is methanogenesis in the active layer (the seasonally thawing soil layer above the permafrost) and that groundwater enriched in CH_4 flows through the active layer before discharging into the lake [*Paytan et al.*, 2015]. In this subsequent study, we use a suite of isotopes in CH_4, water (H_2O), and dissolved inorganic carbon (DIC) to determine the processes controlling CH_4 concentration in the saturated zone of the active layer surrounding Toolik Lake (including but not limited to methanogenesis). We also compare the importance of this CH_4 source to CH_4 diffusing from deep lake sediments, another important source of dissolved CH_4 to the lake [*Cornwell and Kipphut*, 1992]. Understanding the relative importance of these CH_4 sources to Toolik Lake will improve estimates of CH_4

21698961, 2017, 4, Downloaded from https://agupubs.onlinelibrary.wiley.com/doi/10.1002/2016JG003491 by National Central University, Wiley Online Library on [23/02/2023]. See the Terms and Conditions (https://onlinelibrary.wiley.com/terms-and-conditions) on Wiley Online Library for rules of use; OA articles are governed by the applicable Creative Commons License

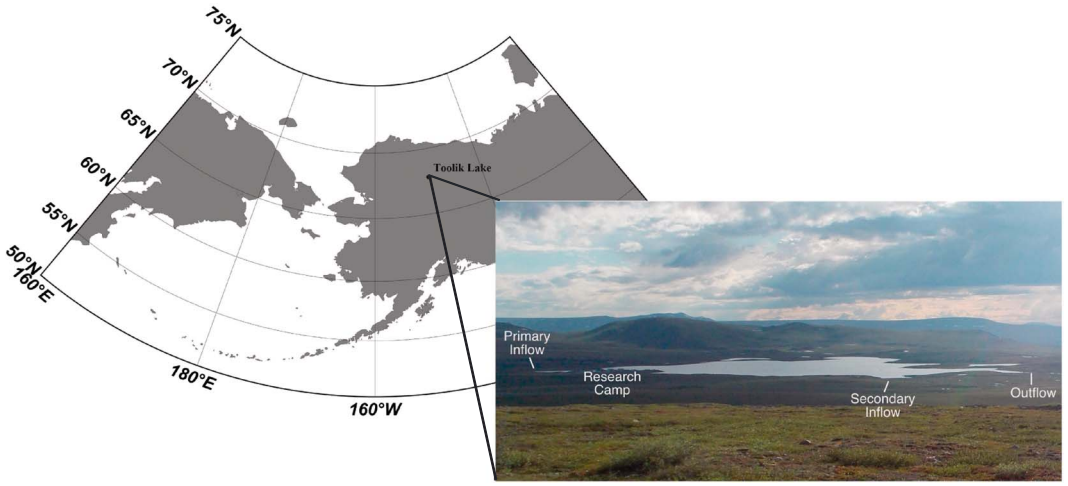

Figure 1. The location of Toolik Lake on the North Slope of Alaska and a south-facing photo with main features of the lake labeled. Map made using Schlitzer, R., Ocean Data View, http://odv.awi.de, 2015.

fluxes from other similar Arctic lakes and contribute to better constraining the global methane budget in the face of a changing climate. Specifically, we discuss how a changing climate may affect CH_4 concentrations in the active layer surrounding Toolik Lake, ultimately affecting the concentration of CH_4 in the groundwater and hence in the lake and related efflux from the lake to the atmosphere.

CH_4 production in terrestrial freshwater systems can occur via two main pathways, acetate fermentation (equation (1)), and CO_2 reduction (equation (2)) [*Chanton*, 2005; *Whiticar et al*., 1986; *Whiticar*, 1999]:

$$CH_3COOH \rightarrow CH_4 + CO_2 \quad (1)$$

$$CO_2 + 4H_2 \rightarrow 2H_2O + CH_4 \quad (2)$$

CH_4 can be oxidized before emission to the atmosphere, a process which depends on the availability of electron acceptors [*Brune et al*., 2000; *King*, 1992; *Segarra et al*., 2013].

Stable isotopic signatures of CH_4 can be used to understand sources and sinks of CH_4 and help define the relative importance of different processes affecting CH_4 production/consumption and their contribution to the methane budget. The two pathways of microbial CH_4 production in low-temperature environments can be distinguished by carbon ($^{13}C/^{12}C$) and hydrogen (D/H) isotope ratios of methane: $\delta^{13}C\text{-}CH_4$: −60 to −110‰ and $\delta D\text{-}CH_4$: −170 to −250‰ for CO_2 reduction, and $\delta^{13}C\text{-}CH_4$: −50 to −60‰ and $\delta D\text{-}CH_4$: −250 to −400‰ for acetate fermentation [*Whiticar*, 1999]. CH_4 produced from acetate fermentation is relatively ^{13}C enriched and δD depleted relative to CH_4 produced from CO_2 reduction [*Chanton*, 2005; *Coleman et al*., 1981]. Isotope signatures from CH_4 sources may be altered by secondary effects such as substrate depletion and CH_4 oxidation [*Whiticar*, 1999]. Specifically, CH_4 isotopes ($\delta^{13}C$ and δD) are often controlled by kinetic isotope fractionations, isotope composition of the precursor substrates (CO_2, acetate, and water), H-isotope exchange between CH_4 and water, and H_2 concentrations [*Chanton*, 2005; *Waldron et al*., 1999; *Whiticar*, 1999]. For example, a previous study showed that $\delta D\text{-}CH_4$ in Alaska is influenced by the δD of formation water [*Brosius et al*., 2012]. However, the formation water may be different from modern precipitation if the source is permafrost or ground ice water from the Pleistocene, although this influence is mostly observed in thermokarst lakes [*Brosius et al*., 2012].

An important functional relationship of low-temperature CH_4 geochemistry is that in a $\delta D\text{-}CH_4$ versus $\delta^{13}C\text{-}CH_4$ diagram, a positive slope reflects methane oxidation and a negative slope reflects CH_4 production [*Chanton et al*., 2005; *Walter et al*., 2008a]. Another important functional relationship is shown in a $\delta D\text{-}CH_4$ versus $\delta D\text{-}H_2O$ diagram where a slope of 1 is expected for CO_2 reduction and a slope of 0.25 for acetate fermentation according to the amount of hydrogen derived from environmental H_2O [*Whiticar et al*., 1986; *Whiticar*, 1999]. Here we take advantage of these relationships to investigate the relative contribution of CH_4 sources to Toolik Lake, Alaska, and to shed light on the processes that currently or may in the future affect these CH_4 inputs into the lake.

Toolik Lake is an oligotrophic kettle lake in the continuous permafrost zone on the North Slope of Alaska (Figure 1), with a maximum permafrost depth of ~0.5 m in its 65 km^2 watershed [*Whalen and Cornwell*,

21698961, 2017, 4, Downloaded from https://agupubs.onlinelibrary.wiley.com/doi/10.1002/2016JG003491 by National Central University, Wiley Online Library on [23/02/2023]. See the Terms and Conditions (https://onlinelibrary.wiley.com/terms-and-conditions) on Wiley Online Library for rules of use; OA articles are governed by the applicable Creative Commons License

21698961, 2017, 4, Downloaded from https://agupubs.onlinelibrary.wiley.com/doi/10.1002/2016JG003491 by National Central University, Wiley Online Library on [23/02/2023]. See the Terms and Conditions (https://onlinelibrary.wiley.com/terms-and-conditions) on Wiley Online Library for rules of use; OA articles are governed by the applicable Creative Commons License

1985]. Deep lake sediments at Toolik Lake are iron rich with low organic matter content, low sedimentation rates, and low oxygen consumption rates [*Cornwell and Kipphut*, 1992]. The perimeter of the lake is surrounded by acidic tundra soil underlain mostly by colluvial and glaciofluvial deposits with organic deposits in the low-lying areas [*Walker and Balser*, 2004]. Hydrologically, the lake has two main rivers entering it and one outflow (Figure 1), although smaller entrainments of runoff enter the lake as well. Precipitation in this region is low with rain occurring only in the summer and averaging 100–200 mm per year [*Kling et al*., 1992; *Whalen and Cornwell*, 1985]. In most years precipitation roughly equals evaporation [*Whalen and Cornwell*, 1985]. Methane evasion via ebullition has not been observed at Toolik Lake, and methane efflux to the atmosphere is dominated by diffusion [*Walter et al*., 2008b]. Toolik Lake and the surrounding areas are managed by the Bureau of Land Management for research purposes of the Long Term Ecological Research Station (LTER). To minimize human impact on the area, all waste and wastewater are trucked offsite to ensure pristine conditions in which to conduct research.

2. Methods

2.1. Discrete Water Sampling

Lake water, groundwater, and river water samples were collected over three field campaigns in July 2012, September 2013, and July 2014. Lake surface water samples were collected from the interior of the lake and the lake perimeter. Water samples from the active layer (referred to here as groundwater samples) were collected from around the lake shoreline by installing temporary well points. Well points were installed by digging into the tundra until reaching permafrost (typically < 0.5 m), inserting screened well points and allowing the system to equilibrate for several hours. Before collection, water equivalent to two well volumes was pumped out to ensure the sample was collected from the active layer and not from standing water in the well. Submersible pumps were lowered to the deepest point in the well for sample collection, and water collected at the minimal volumes needed for analysis to prevent overt drawdown of the well. Groundwater samples were also collected from the thaw bulb below the lake using the Toolik Lake Long Term Ecological Research Station's (LTER) camp water supply well (depth ~ 39.9 m). River water samples were collected from the primary and secondary inflows into Toolik Lake. Lake depth profile samples were collected at three locations in 2013, which were repeated in 2014. Profile 1 was located in the center of the lake, profile 2 was located closest to the secondary inflow, and profile 3 was located near the northwest inlet of the lake. Specific conductivity and temperature of all samples were measured with a handheld YSI 85 multiprobe.

2.2. CH_4 Concentration and Isotopes

Groundwater and lake water samples were collected into glass bottles (125 ml and 160 ml Wheaton bottles, respectively) for CH_4 concentration and isotope analyses. Groundwater samples were collected in triplicate, and lake water samples were collected in duplicate. Typically, all the volume in a bottle was needed for each isotopic analysis for lake water (e.g., one bottle used for concentration and δD-CH_4 and one for δ^{13}C-CH_4) due to the low concentrations in the lake and the minimum amount of methane requirements for each analysis. Dissolved CH_4 concentrations in water samples were measured using a headspace equilibration technique [*Magen et al*., 2014]. Water samples were collected by direct filling of the glass serum bottles at a flow rate of less than 100 mL min^{-1}, allowing the vials to overflow three times. The serum bottles were sealed without headspace using blue butyl stoppers, and saturated $HgCl_2$ solution (0.3 mL) was added immediately after sample collection to halt biological activity. Before analysis, 10% of the water sample volume was removed, and replaced by the same volume of helium gas to create a headspace. Sample vials were shaken vigorously for 3 min and placed on a shaker for 30 min at room temperature (25°C).

CH_4 concentrations for all samples were measured on an SRI 310 Gas Chromatograph (GC) equipped with a flame ionization detector and an Alltech Haysep S 100/120 column (6′ × 1/8″ × 0.085″). A volume of 0.25 mL of gas was removed from the headspace with a syringe for analysis, and the same volume of CH_4 free Milli-Q water was injected to replace the volume of the gas removed. Helium was used as the carrier gas at a flow rate of 15 mL min^{-1}, and the column and detector temperatures were maintained at 50°C and 150°C, respectively. Peak integration was performed using Peak Simple NT software. Gas mixtures used for GC calibration and standard curves were made using successive dilutions of 1000 ppm CH_4. Total CH_4 concentration in the water samples was calculated by adding the measured headspace CH_4 concentration and the amount of CH_4

21698961, 2017, 4, Downloaded from https://agupubs.onlinelibrary.wiley.com/doi/10.1002/2016JG003491 by National Central University, Wiley Online Library on [23/02/2023]. See the Terms and Conditions (https://onlinelibrary.wiley.com/terms-and-conditions) on Wiley Online Library for rules of use; OA articles are governed by the applicable Creative Commons License

remaining in the water sample after headspace equilibration, calculated from the solubility equation of *Yamamoto et al*. [1976]. The average combined standard error of sampling and analysis was 3.6% ($n = 27$).

After CH_4 concentration analysis, the remaining headspace gas samples were injected into 10 mL exetainers for $\delta^{13}C$-CH_4 and δD-CH_4 analysis. One exetainer was required for each isotopic analysis. δD-CH_4 was analyzed at the University of California Davis Stable Isotope Facility on a ThermoScientific PreCon concentration system interfaced to a ThermoScientific Delta V Plus isotope ratio mass spectrometer (ThermoScientific, Bremen, DE) [*Yarnes*, 2013]. $\delta^{13}C$-CH_4 was analyzed at the Lawrence Livermore National Laboratory using the standard TraceGas preconcentration system interfaced with an IsoPrime isotope ratio mass spectrometer (IsoPrime Ltd, UK) as described by *Fisher et al*. [2006]. The mass requirements for $\delta^{13}C$-CH_4 and δD-CH_4 analyses were 10 nmol and 2 nmol, respectively. Hence, samples with very low concentrations were not analyzed for isotope ratios.

2.3. Isotopes in DIC

For stable carbon isotope of DIC analysis, water samples were collected using the same method as CH_4 samples into 40 mL glass vials. A 10 mL aliquot of sample water was taken out of the vials and replaced with 10 mL of helium using a three-way valve needle attached to a helium gas cylinder. After filling the syringe with 10 mL of He, the syringe was injected into a preplaced rubber septa above the sample vial septa to occlude air from the needle. The needle was injected into the sampling vial, and He was slowly injected by pressing the plunger. Acid (0.5 mL of 6 M HCl) was injected to convert DIC to CO_2. Vials were shaken for 30 s using a vortexer to let CO_2 equilibrate. This was done for both samples and standards.

A 1 mL subsample of the headspace gas was then injected into a Carlo Erba NA 1500 elemental analyzer with Micromass Optima continuous flow mass spectrometer at the U.S. Geological Survey (USGS), Menlo Park, CA for DIC carbon isotopic composition measurements. External standards of sodium bicarbonate ($NaHCO_3$) and potassium carbonate (K_2CO_3) dissolved in CO_2-free Milli-Q water were also analyzed. The $\delta^{13}C$ values of repeated analyses of the K_2CO_3 and $NaHCO_3$ standards are -25.85 ± 0.35‰ ($n = 9$) and -5.77 ± 0.18‰ ($n = 9$), respectively. Carbon isotope values are reported in delta notation ($\delta^{13}C$) relative to the Vienna PeeDee Belemnite standard. Carbon isotopes in DIC analysis was only conducted on a small subset of groundwater samples.

2.4. Isotopes in Water

Water samples for δD-H_2O and $\delta^{18}O$-H_2O were collected by submersible pump in concert with CH_4 concentration samples in 2012 and 2014 and filtered to 0.45 μm into 2 mL gas chromatography vials. Samples were analyzed at the UC Davis Stable Isotope Facility on a Laser Water Isotope Analyzer V2 (Los Gatos Research Inc.). Precision is typically ≤0.3‰ for $\delta^{18}O$-H_2O and ≤0.8‰ for δD-H_2O. Values are reported relative to Vienna SMOW.

3. Results

Results of δD-H_2O and $\delta^{18}O$-H_2O are shown in Figure 2. For both years lake and river water samples fell to the right of the Global Meteoric Water Line (GMWL), on a line typical of evaporation in surface water bodies [*Gat*, 1996]. The shift was smaller in 2014, indicating either more precipitation that year or less evaporation. Thaw bulb samples likewise fell in the vicinity of the surface water samples, shifted to the right of the GMWL. In 2012 groundwater samples clustered as two groups along the GMWL, to the right and left of surface water samples (lake and river). A similar pattern was shown by the 2014 groundwater samples, although the isotope range represented by these samples was muted compared to 2012.

Depth profiles of temperature, CH_4 concentration, $\delta^{13}C$-CH_4, and δD-CH_4 at three locations in the lake from 2013 (September) and 2014 (June) are shown in Figure 3. In 2013 temperature was uniform with depth, indicating a well-mixed lake, while in 2014 temperature was warmest at the surface and decreases with depth indicating seasonal stratification. CH_4 concentrations were uniformly low (<250 nM) during mixed conditions (September 2013), while during stratification (June 2014) CH_4 was low near the surface (~250 nM) and increased with depth (up to 350 nM). $\delta^{13}C$-CH_4 and δD-CH_4 profiles from 2013 to 2014 were generally uniform with depth (-60.3‰ $\pm$ 0.7‰ for $\delta^{13}C$-CH_4 and -273‰ $\pm$ 4‰ for δD-CH_4), with a few random less negative values. Profile 3 in 2014 shows lighter isotope ratios for both isotopes near the surface (-63‰ for $\delta^{13}C$-CH_4 and -305‰ for δD-CH_4) shifting toward heavier isotopes below 10 m depth (-50‰ and -209‰ at depth, respectively).

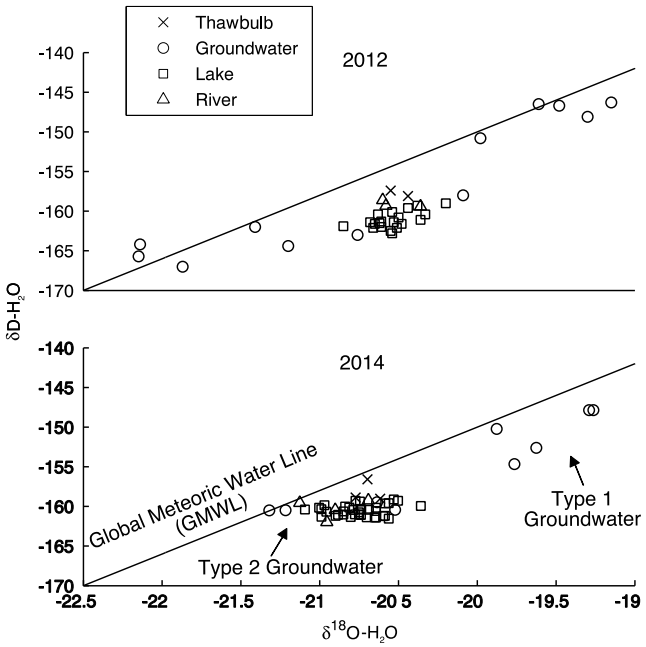

Figure 2. δD-H_2O and δ^{18}O-H_2O (top) for 2012 and (bottom) 2014 in lake water, groundwater, river water, and from the thaw bulb. The solid line is the global meteoric water line. Groundwater generally falls on the Global Meteoric Water Line GMWL with surface water bodies (river and lake water) deviating from the GMWL on an evaporation line. Thaw bulb samples fall likewise on the evaporation line, indicating surface water sources recharge it.

Plots of δD-CH_4 versus δ^{13}C-CH_4 for all samples are shown in Figure 4. Thaw bulb samples clustered in the carbonate reduction area, while groundwater samples from the active layer and lake margin sediments clustered in either the bacterial methyl-type fermentation area or along adjacent CH_4 oxidation pathways [*Whiticar*, 1999]. Lake and river samples fell between these three end-members. The atmospheric CH_4 sample plotted as expected in the isotopically heavier area of the plot, while pore water from shallow lake sediments, collected close to the lake perimeter, plotted near the bacterial methyl-type fermentation, similar to most of the active layer groundwater samples.

Maps of the spatial distribution of δ^{13}C-CH_4 and δD-CH_4 in Toolik Lake area for 2013 and 2014 are shown in Figure 5. Groundwater isotope ratios varied largely at the local scale, for example, two groundwater samples collected from the same area

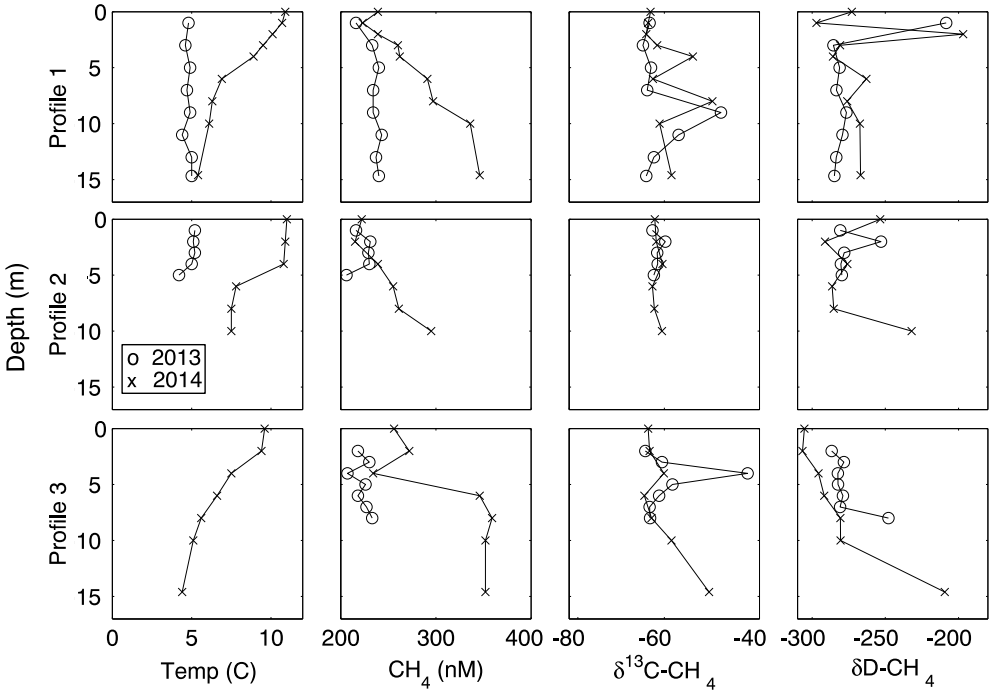

Figure 3. Depth profiles for three locations within the lake (profiles 1, 2, and 3; locations shown on Figure 5) for 2013 and 2014 for (first column) temperature, (second column) CH_4 concentration, (third column) δ^{13}C-CH_4, and (fourth column) δD-CH_4. The *Y* axis is depth in meters.

21698961, 2017, 4, Downloaded from https://agupubs.onlinelibrary.wiley.com/doi/10.1002/2016JG003491 by National Central University, Wiley Online Library on [23/02/2023]. See the Terms and Conditions (https://onlinelibrary.wiley.com/terms-and-conditions) on Wiley Online Library for rules of use; OA articles are governed by the applicable Creative Commons License

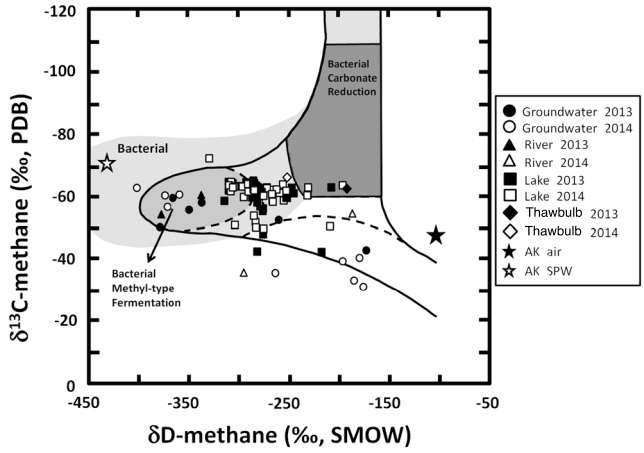

Figure 4. Diagram for classification of methane by δD-CH_4 and δ^{13}C-CH_4 values in all samples (zones defined from *Whiticar* [1999]). Thaw bulb samples cluster in the carbonate reduction zone. Groundwater and shallow sediment pore water (AK SPW) cluster in the bacterial methyl type fermentation or on an oxidation trend toward heavier values in both isotopes. Lake water samples cluster between these two groups.

(northwest) in 2014 encompassed almost the whole range of δD-CH_4 (-175‰ to -400‰) for the whole data set. While groundwater samples showed large heterogeneity, lake samples fell into two groups. Interior lake samples were more homogeneous and lighter in δ^{13}C-CH_4 and δD-CH_4 than perimeter lake samples (samples within 50 m of shore), which were isotopically heavier and more heterogeneous.

A plot of δ^{13}C-CH_4 against δ^{13}C-DIC is shown in Figure 6. This plot subsists of a subsample of data from Figure 4. Thaw bulb data and most groundwater data clustered, as they did with the CH_4 isotopes, in the carbonate reduction and methyl-type fermentation pathways (see Figure 4), respectively. Samples that clustered more toward the methane oxidation area in Figure 4 also fell in the methane oxidation area based on δ^{13}C-DIC.

4. Discussion

4.1. Processes Governing CH_4 Concentrations in and Around Toolik Lake

Based on the isotope data, CH_4 concentration, and hydrological characteristics, we categorize all samples into four distinct groups: lake water, thaw bulb water, Type 1 groundwater, and Type 2 groundwater. The combination of low CH_4 concentrations of river water, some samples even lower than lake water, and estimated river discharge into the lake begets a relatively low CH_4 contribution to the lake via this pathway and is not further considered here as a major CH_4 source to the lake at the time of our study [*Whalen and Cornwell*, 1985]. CH_4 concentration, δ^{13}C-CH_4, and δD-CH_4 for each group are summarized in Table 1, along with significant differences (two-tailed t test assuming unequal variances; $p < 0.1$) between groundwater types when enough sample data were available ($n \geq 3$). CH_4 concentrations in lake water (surface samples and depth profiles; 141 to 1151 nM) are lower than the concentration in the previously identified external sources of CH_4 to the lake, groundwater (90 to 22,120 nM), and thaw bulb samples (1951–8610 nM). The δ^{13}C-CH_4 and δD-CH_4 data for the lake samples (-73 to -42‰ and -331 to -197‰, respectively) plot between the methyl-type fermentation and carbonate-reduction pathways (Figure 4). With respect to isotopes in water (Figure 2), lake water samples lay on an evaporation line off the global meteoric water line (GMWL) due to isotopic fractionation during evaporation. Groundwater samples fall close to the GMWL as they are less affected by evaporation. While the GMWL has a slope of about 8 (8 δD: 1 δ^{18}O), evaporation lines have a slope less than 8, typically between 4 and 6 (4 to 6 δD: 1 δ^{18}O) [*Gibson et al.*, 1993]. Indeed, the slope of surface water samples in this instance is 4 in 2012. A slope cannot be determined for 2014 due to the low fit ($R^2 = 0.03$) of the trend line to the surface water samples of that year. The poor correlation may be due to uneven evaporation across the collection sites or different sources of water, such as permafrost meltwater, disrupting the signal.

21698961, 2017, 4, Downloaded from https://agupubs.onlinelibrary.wiley.com/doi/10.1002/2016JG003491 by National Central University, Wiley Online Library on [23/02/2023]. See the Terms and Conditions (https://onlinelibrary.wiley.com/terms-and-conditions) on Wiley Online Library for rules of use; OA articles are governed by the applicable Creative Commons License

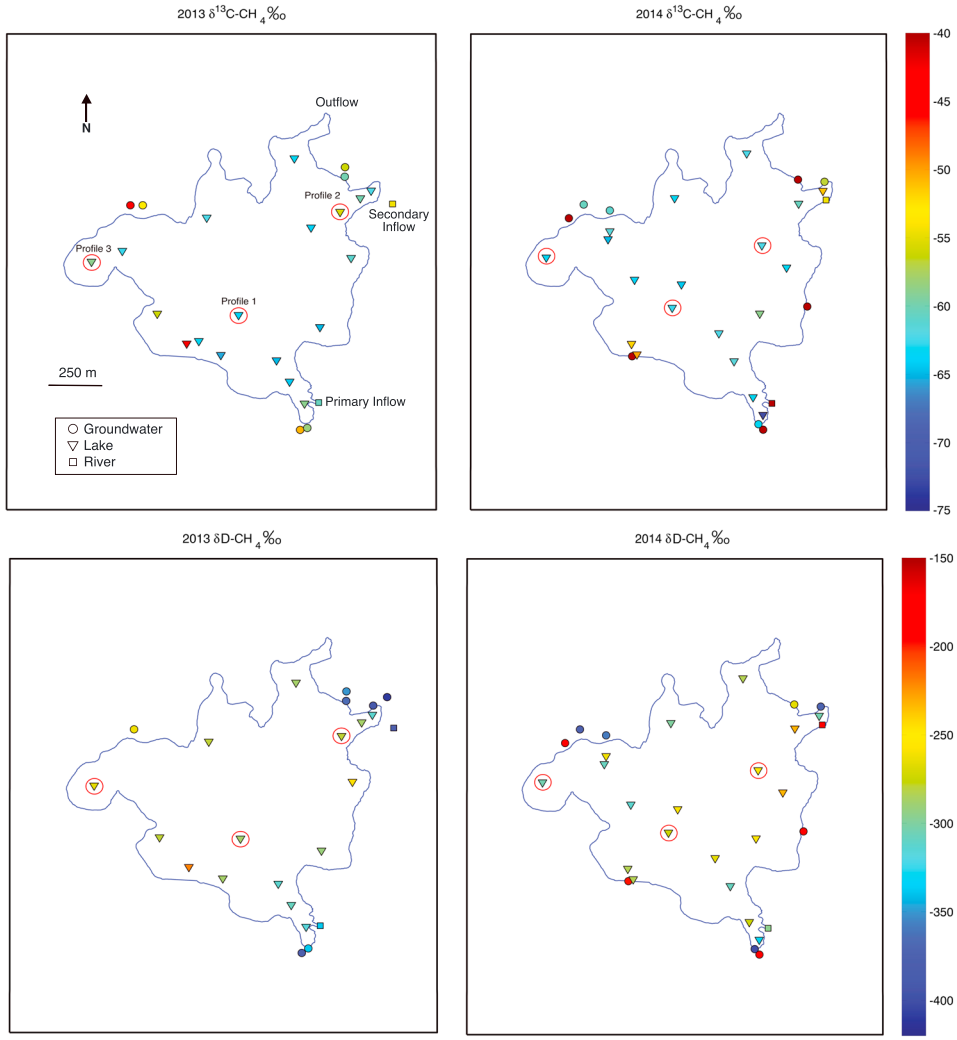

Figure 5. Maps of surface water sample locations for (top row) δ^{13}C-CH_4 and (bottom row) δD-CH_4 for (left column) 2013 and (right column) 2014. Red circles indicate depth profile locations. Profile 1 was located in the center of the lake, profile 2 was located closest to the secondary inflow, and profile 3 was located in the northwest inlet of the lake.

Thaw bulb water has similar δD-H_2O and δ^{18}O-H_2O as the lake water (Figure 2) suggesting recharge of the thaw bulb from the lake above, recharge that occurs when water is drawn out of the thaw bulb by the Toolik Lake LTER camp well, the only means of filling the daily water needs of 200+ scientist and support staff at the Toolik Lake LTER. With respect to the CH_4 isotopic compositions, samples from the thaw bulb (−66 to −63‰ and −252 to −193‰ for δ^{13}C and δD, respectively) are distinct from the groundwater samples in that they cluster within the carbonate reduction end-member of the δ^{13}C-CH_4 and δD-CH_4 cross plots (Figure 4) and are high in CH_4, with a median of 1921 nM (1950 to 8610 nM).

Types 1 and 2 groundwater were determined based on geochemical characteristics. The water isotopes of Type 1 groundwater cluster on the isotopically heavier portion of Figure 2 indicating this water precipitated during a warmer period (summer), likely as rain [*Gat*, 1996]. Type 1 groundwater wells had higher CH_4 concentrations (540 to 22,100 nM) than Type 2 groundwater and in Figure 4 cluster within the methyl-type bacterial fermentation zone (−63 to −50‰ and −411 to −338‰ for δ^{13}C and δD, respectively). This is also near the values of the shallow perimeter lake sediment pore water. Type 1 groundwater samples can be identified by the blue (nonred/nonyellow) markers (indicating methyl-type bacterial fermentation) on the δD plots of Figure 5. Type 1 groundwater is similar in characteristics to shallow perimeter lake sediment pore water, and both water types experience similar conditions within the sediment, such as a thick saturated zone.

21698961, 2017, 4, Downloaded from https://agupubs.onlinelibrary.wiley.com/doi/10.1002/2016JG003491 by National Central University, Wiley Online Library on [23/02/2023]. See the Terms and Conditions (https://onlinelibrary.wiley.com/terms-and-conditions) on Wiley Online Library for rules of use; OA articles are governed by the applicable Creative Commons License

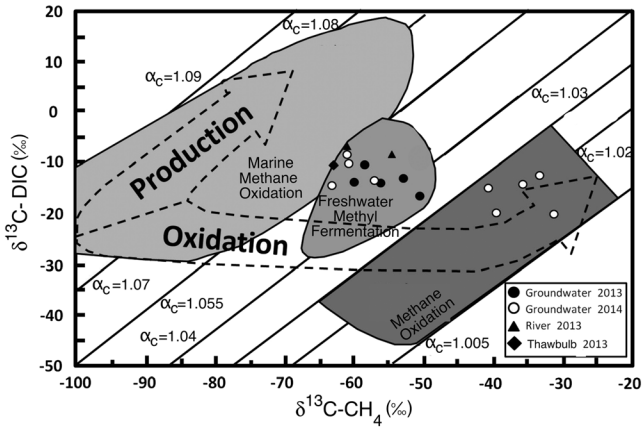

Figure 6. δ^{13}C-CH_4 versus δ^{13}C-DIC for 2014 (zones determined from *Whiticar* [1999], with isotope fractionation lines (αc). Thaw bulb data and most groundwater data cluster as they did in the carbonate reduction and methyl-type fermentation pathways of Figure 4, respectively. Samples which clustered more toward CH_4 oxidation associated area of Figure 4 here fall in the CH_4 oxidation area too.

Type 2 groundwater displayed different geochemical characteristics than Type 1 groundwater. The isotopically lighter signatures of the water isotopes (Figure 2) of Type 2 groundwater indicates the source of this water precipitated during colder periods (fall, winter, and spring) likely as snow. The strong evaporation trend in the samples that overlie the surface water samples is consistent with a lot of evaporation in a thin saturated zone [*Gat*, 1996]. Type 2 groundwater samples were lower in CH_4 concentration, with a median of 165 nM (90 to 206 nM) and fell within the CH_4 oxidation pathway zone of Figure 4 (e.g., have higher isotope ratios, −53 to −31‰ and −264 to −173‰, for δ^{13}C and δD,

Table 1. Average With Standard Error, Range, and Number of Samples for CH_4 Concentration, δ^{13}C-CH_4, and δD-CH_4 in Types 1 and 2 Groundwater, Lake Water, River Water, and Thaw Bulb Water

	CH_4 (nM)	δ^{13}C-CH_4	δD-CH_4
	2013		
Type 1 Groundwater	5,000 ± 3000 [575 − 22,120] *n* = 6	−56 ± 14 [−60 − −50] *n* = 4	−373 ± 2 [−411 − −338] *n* = 6
Type 2 Groundwater	205 ± 17 [188–222] *n* = 2	−48 ± 44 [−53 − −43] *n* = 2	−217 ± 4 [−261 − −173] *n* = 2
Lake Water	232 ± 7 [150 − 385] *n* = 35	−60 ± 4 [−65 − −42] *n* = 35	−278 ± 1 [−315 − −208] *n* = 35
Thaw bulb	1,951 *n* = 1	−63 *n* = 1	−193 *n* = 1
Rivers	350 ± 10 [331 − 358] *n* = 2	−60 ± 20 [−60 − −54] *n* = 2	−358 ± 3 [−379 − −338] *n* = 2
	2014		
Type 1 Groundwater*	2,000 ± 1000 [540 − 6,820] *n* = 4	−60 ± 1 [−63 − −57] *n* = 4	−380 ± 9 [−408 − −360] *n* = 4
Type 2 Groundwater*	130 ± 20 [90 − 206] *n* = 5	−36 ± 2 [−41 − −31] *n* = 5	−201 ± 16 [−264 − −176] *n* = 5
Lake Water	290 ± 20 [141 − 1151] *n* = 38	−61 ± 1 [−73 − −50] *n* = 38	−276 ± 4 [−331 − −197] *n* = 38
Thaw bulb	8,100 ± 300 [7,530 − 8,610] *n* = 3	−66 *n* = 1	−252 *n* = 1
Rivers	168 ± 15 [133 − 205] *n* = 4	−45 ± 9 [−55 − −36] *n* = 2	−240 ± 50 [−296 − −187] *n* = 2

*Two-tailed *t* test assuming unequal variances showed significant differences in CH_4, δ^{13}C-CH_4, and δD-CH_4 between Types 1 and 2 groundwater in 2014 ($p < 0.1$).

21698961, 2017, 4, Downloaded from https://agupubs.onlinelibrary.wiley.com/doi/10.1002/2016JG003491 by National Central University, Wiley Online Library on [23/02/2023]. See the Terms and Conditions (https://onlinelibrary.wiley.com/terms-and-conditions) on Wiley Online Library for rules of use; OA articles are governed by the applicable Creative Commons License

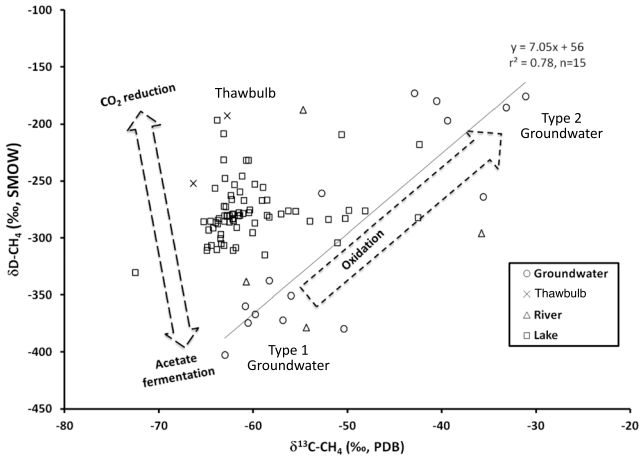

Figure 7. Plot of δD-CH_4 versus δ^{13}C-CH_4 for all samples. The line is a regression of groundwater samples. Plot areas where Type 1 groundwater, Type 2 groundwater, and thaw bulb data are located are labeled. Most lake samples fall between the thaw bulb and Type 1 groundwater end-members.

respectively). Figure 6 (cross plots of δ^{13}C-DIC and δ^{13}C-CH_4) also shows these samples lie within an area of the plot defined by CH_4 oxidation as this process enriches the residual CH_4 with the heavier isotopes. δ^{13}C-CH_4 controlled by CH_4 oxidation in the Type 2 groundwater is further supported by the positive slope of 7.05 of the groundwater δ^{13}C-CH_4 and δD-CH_4 (Figure 7). Indeed, the occurrence of aerobic CH_4 oxidation is suggested by a positive correlation between δD-CH_4 and δ^{13}C-CH_4 with a slope of 5 to 13.5 [*Coleman et al*., 1981; *Happell et al*., 1994; *Powelson et al*., 2007]. The differences in CH_4 concentration, in δ^{13}C, and δD in CH_4 of Type 2 groundwater were statistically different from Type 1 groundwater in 2014; not enough samples were collected in 2013 to perform hypothesis testing using statistics.

The combination of isotopically lighter CH_4 and higher CH_4 concentration in the Type 1 groundwater and of isotopically heavier CH_4 and lower CH_4 concentration in the Type 2 groundwater along with the detection of CH_4 oxidation in the Type 2 groundwater indicates that distinct conditions within the active layer of these two groundwater types affect the CH_4 concentrations. In Type 1 groundwater methanogenesis rates are high, and oxidation rates are low, as indicated by the high CH_4 concentrations in these samples (5000 ± 3000 nM in 2013 and 2000 ± 1000 nM in 2014), possibly due to a thicker saturated zone that allows anoxia to develop. This process is similar to the development of anoxic zones in highly stratified lakes and fjords [*Comeau et al*., 2012; *Pawlowicz et al*., 2007]. Methanogenesis by the methyl-type pathway (lighter isotopes) is fueled by high concentrations of organic matter, while water from rain (inferred from the water isotopes) ensures the saturated layer remains anoxic. Conversely, much of the CH_4 in Type 2 groundwater samples is sourced from bacterial methyl fermentation type pathways, and some of this CH_4 is oxidized leaving low CH_4 concentrations that are isotopically heavy. Therefore, we interpret Type 2 groundwater as being the residual of Type 1 groundwater after considerable CH_4 oxidation (both produced by the methyl-type pathway).

Due to the fully saturated state of the shallow lake sediments (e.g., submerged) and the relatively high organic matter content there compared to the deeper-lake sediments (our observation of large amounts of dead organic matter in the shallow sediments and as reported in *Cornwell and Kipphut* [1992]), similar processes occur there as in the Type 1 groundwater. An anoxic zone develops, leading to methanogenesis by the methyl-type pathway and clustering along with Type 1 groundwater samples on the CH_4 dual isotope plot (Figure 4). Since these two water types, Type 1 groundwater and shallow lake sediment pore water, are dominated by the same processes, and the CH_4 in these samples is isotopically similar and impossible to distinguish between the two using CH_4 isotopes alone.

4.2. CH_4 Sources to Toolik Lake

CH_4 from external sources such as groundwater and production in deep lake sediments have been identified as potential sources of CH_4 to Toolik Lake [*Cornwell and Kipphut*, 1992; *Paytan et al*., 2015]. We identify three

21698961, 2017, 4, Downloaded from https://agupubs.onlinelibrary.wiley.com/doi/10.1002/2016JG003491 by National Central University, Wiley Online Library on [23/02/2023]. See the Terms and Conditions (https://onlinelibrary.wiley.com/terms-and-conditions) on Wiley Online Library for rules of use; OA articles are governed by the applicable Creative Commons License

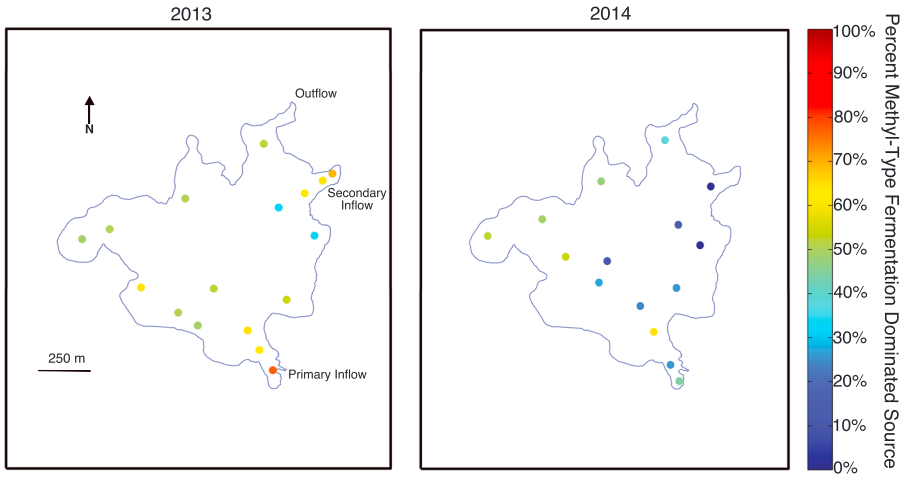

Figure 8. Spatial mixing model results by percent of methyl-type dominated sources (Type 1 groundwater and shallow perimeter lake sediments. The 100% represents all methyl-type dominated sources, and 0% represents all bacterial carbonate reduction sources (thaw bulb) for (left) 2013 and (right) 2014. The lake perimeter shows more methyl-type dominated sources while the interior of the lake shows more bacterial carbonate reduction influence.

different water types that contribute CH_4 to the lake (Type 1 groundwater and shallow perimeter lake sediments, Type 2 groundwater, and thaw bulb) clustering as different end-members on Figure 4 (bacterial methyl-type, methane oxidation, and bacterial carbonate reduction). Lake water lies between the three end-members, although somewhat more between Type 1 groundwater and the thaw bulb water (the two bacterial pathways). Thus, it appears that CH_4 in the lake may be a mix of CH_4 from all these end-members. However, Type 2 groundwater is probably not an important source of groundwater and associated CH_4 to the lake, due to the orders of magnitude lower CH_4 concentrations in Type 2 groundwater (and therein the CH_4 oxidation end-member). Additionally, the low CH_4 concentrations in rivers (Table 1) make them a minor contributor to the Toolik Lake CH_4 budget. Therefore, we focus our discussion on the two remaining end-members identified in Figure 4, specifically Type 1 groundwater (including shallow perimeter lake sediments) produced through bacterial methyl fermentation and deep lake sediments (thaw bulb) dominated by bacterial carbonate reduction and their relative importance to CH_4 in Toolik Lake.

To determine the importance of CH_4 delivered from sources dominated by methyl-type fermentation (MTF) and CH_4 from sources dominated by bacterial carbonate reduction (BCR) to the CH_4 inventory of Toolik Lake, we employ a mixing model for groundwater using δ^{13}C-CH_4 and δD-CH_4 modified from *Lecher et al.* [2016].

$$GC_g + TC_t = C_l \quad (4)$$

$$GH_g + TH_t = H_l \quad (5)$$

G and T are the fractions of CH_4 from MTF or BCR in Toolik Lake; C_g, C_t, and C_l are the δ^{13}C-CH_4 of MTF-dominated sources, BCR-dominated sources, and lake water, respectively; and H_g, H_t, and H_l are the fractions of δD-CH_4 of MTF-dominated sources, BCR-dominated sources, and lake water, respectively. The mixing model was solved for each data point representing surface lake water (Figure 8) and water from the depth profiles (Figure 9), with MTF-dominated source values, and BCR-dominated sources, as reported in Table 1 averages. The mixing model was not calculated for any data points (surface lake water and depth profiles) that appear to have undergone any amount of CH_4 oxidation (δD-$CH_4 > -275$) as this data are not well represented by the mixing model.

Within the surface water data of Toolik Lake MTF-dominated sources are more prominent near the perimeter of the lake in both years (40% to 90% groundwater CH_4 in 2013 and 40% to 70% groundwater CH_4 in 2014). In contrast, the BCR-dominated sources are more prevalent in the center of the lake (40% to 50% groundwater CH_4 in 2013 and 0% to 50% groundwater CH_4 in 2014). This is to be expected as the MTF-dominated sources (Type 1 groundwater and near-shore sediments) enter the lake from the active layer and shallow lake sediments at the lake perimeter. Away from the perimeter of the lake, the BCR-dominated sources (deep

21698961, 2017, 4, Downloaded from https://agupubs.onlinelibrary.wiley.com/doi/10.1002/2016JG003491 by National Central University, Wiley Online Library on [23/02/2023]. See the Terms and Conditions (https://onlinelibrary.wiley.com/terms-and-conditions) on Wiley Online Library for rules of use; OA articles are governed by the applicable Creative Commons License

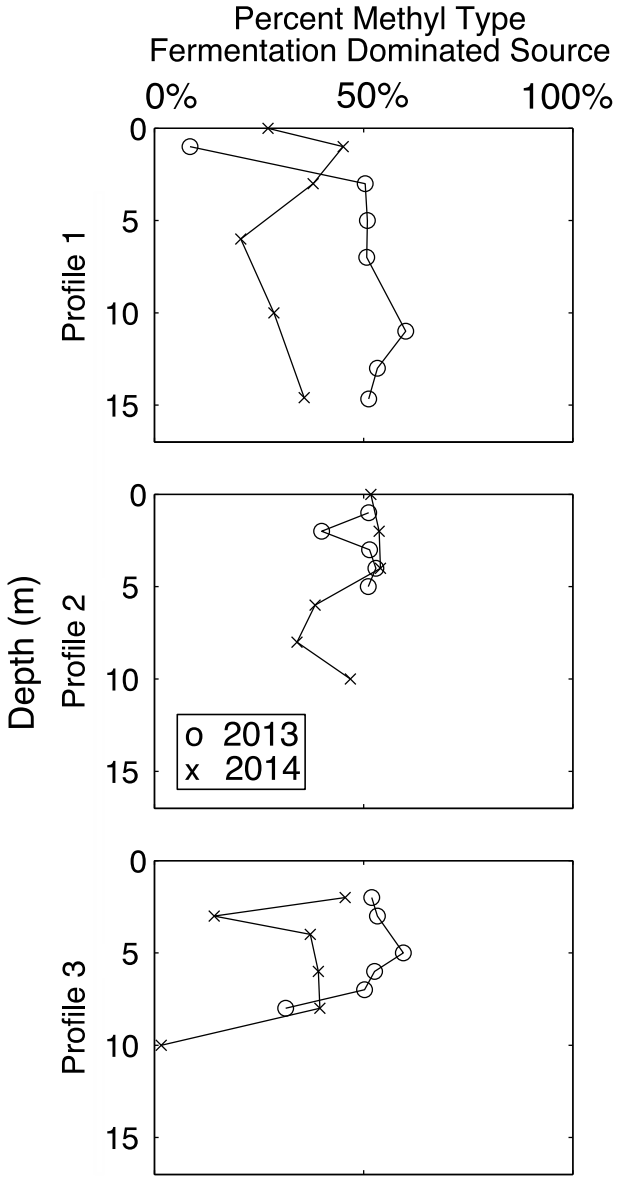

Figure 9. Depth profile mixing model results, with 100% representing all methyl-type dominated sources and 0% representing all bacterial carbonate reduction source. *Y* axis is depth in meters.

lake sediments/thaw bulb) present a stronger influence, as lake water in this area is further way from the perimeter influence. A previous study of diffusive CH_4 water-air fluxes in Toolik Lake conducted in the summers of 2011 and 2012 found higher CH_4 water to air fluxes close to the perimeter of the lake than in the center [*Garcia-Tigreros Kodovska et al.*, 2016]. This suggests a proportionally larger impact of MTF-dominated sources delivered CH_4 on atmospheric emissions from the lake.

Aside from these general trends, there are also temporal differences in the relative influence of MTF-dominated sources and the deep sediment/thaw bulb CH_4 inputs to the surface of the lake year to year. Data from 2013 show more prevalent MTF-dominated sources (40 to 90% groundwater CH_4) while 2014 show more BCR-dominated sources (0 to 70% groundwater CH_4). We would expect a shift toward MTF-dominated sources (particularly Type 1 groundwater) with increased precipitation. However, we observe the opposite as 2014 had 21% more annual precipitation (237 mm) than 2013 (196 mm) (precipitation data via Toolik Lake tipping bucket from http://toolik.alaska.edu/edc/abiotic_monitoring/data_query.php). This does not negate our hypothesis that more precipitation begets a higher flux to the lake from Type 1 groundwater. The mixing model is dependent not only on the relative contribution of Type 1 groundwater (and shallow perimeter lake sediments) but also the contribution from the thaw bulb (the BCR-dominated source) as well. In 2013 the concentrations of CH_4 in the thaw bulb was much lower (1951 nM) than in 2014 (8110 nM). Higher CH_4 concentrations in the thaw bulb in 2014 will induce a higher flux of CH_4 from the thaw bulb and therein a greater thaw bulb influence. This higher flux may mask the larger Type 1 groundwater input that results from increased precipitation (e.g. a fourfold increase in the concentration of methane in the thaw bulb and only 21% increase in precipitation). The thaw bulb CH_4 concentrations are impacted by the thaw bulb pore water temperatures, with higher temperatures conducive to more CH_4 production. Indeed, the lower CH_4 concentration in 2013 (1951 nM) is accompanied by a lower temperature (2.1°C), while the higher CH_4 concentration of 2014 (8110 nM) is paired with a higher temperature (5.5°C). Methanogenesis decreases with temperature in Arctic lake sediments, accounting for the lower CH_4 concentration in 2013 [*Blake et al.*, 2015]. A scaling analysis of Fick's Law for calculating CH_4 diffusive fluxes from the thaw bulb to the lake supports this conclusion (supporting information) [*Boudreau*, 1997].

21698961, 2017, 4, Downloaded from https://agupubs.onlinelibrary.wiley.com/doi/10.1002/2016JG003491 by National Central University, Wiley Online Library on [23/02/2023]. See the Terms and Conditions (https://onlinelibrary.wiley.com/terms-and-conditions) on Wiley Online Library for rules of use; OA articles are governed by the applicable Creative Commons License

21698961, 2017, 4, Downloaded from https://agupubs.onlinelibrary.wiley.com/doi/10.1002/2016JG003491 by National Central University, Wiley Online Library on [23/02/2023]. See the Terms and Conditions (https://onlinelibrary.wiley.com/terms-and-conditions) on Wiley Online Library for rules of use; OA articles are governed by the applicable Creative Commons License

The depth profiles within the interior of the lake were also evaluated using the mixing model (Figure 9). Results of each profile are similar year to year despite the lake being stratified in 2014 and mixed in 2013. Water at most of the depths is consistent with equal parts of MTF-dominated sources and thaw bulb CH_4, the exceptions being one surface sample from profile 1 and the deepest points of profile 3 that show mostly thaw bulb origin. The strong influence of the thaw bulb CH_4 in the bottom of profile 3 hints at bottom sediments being a source of CH_4 as expected. The surface sample of profile 1 which shows almost all thaw bulb CH_4 influence in 2013 (when the lake was mixed) could be explained by mixing, which results in deep thaw bulb CH_4 reaching the surface, although it is also possible that this data point is not well represented by the model. We are unable to differentiate between the two options.

The largest source of error in the mixing model is the accurate characterization of the thaw bulb end-member, as samples could only be collected from one location in the thaw bulb, the area sampled by the camp well. We assumed homogeneity of isotopes within the thaw bulb. The biggest limitation of this mixing model is its inability to differentiate between CH_4 from Type 1 groundwater that enters the lake from external sources at the perimeter and CH_4 produced in situ in shallow lake sediments, which are both grouped in the same end-member (MTF-dominated sources) in the model due to isotopic similarities. We know from previous studies that at least a portion of the CH_4 flux (0.5 to 2.9 g m^{-2} yr^{-1}) to the lake is from groundwater discharge [*Paytan et al*., 2015], but the benthic flux from shallow lake sediments was not directly quantified.

When considering what changes to the local environment would induce increases or decreases in the amount of CH_4 in the various input sources, the two drivers are an increase/decrease in precipitation and increase/decrease in air temperature. A 50 year analysis of air temperature and precipitation trends in Alaska showed that although temperature significantly increased across most of Alaska precipitation increased (most areas) and decreased (on the Arctic Ocean) depending on location, with the transition somewhere around the Toolik Lake area [*Stafford et al*., 2000]. The dependence of precipitation on air temperature and vice versa is currently unknown for the Toolik Lake area.

An increase in rain could increase the area of Toolik Lake, flooding the perimeter shoreline and saturating the organic-rich sediment, inducing more CH_4 production in those areas (more CH_4 from the MTF pathway). Indeed some lakes in the Arctic have been decreasing in size while others have been increasing [*Anderson et al*., 2013; *Payette et al*., 2004; *Smith et al*., 2005] with implications for changes in this source of CH_4. An increase in rain could also cause an increase in the saturated zone thickness, where a thick saturated zone would beget the formation of an anoxic bottom layer where methanogenesis thrives. This assertion is supported by the water isotopes in Type 1 (high CH_4) areas, which display water isotopic values associated with rain compared to Type 2 (low-CH_4) areas, which display water isotopic values associated with snow (Figure 2). It may be argued that much less water (and therein precipitation) would be needed to increase the saturated zone of the active layer directly around the lake than to overflow and expand the perimeter of the lake, because the pore space of sediment surrounding the lake is so much smaller in volume (porosity of substrate < 0.5) than the amount of water required to raise the lake water level (porosity of air above the lake $= 1$). This may be especially true because the outflow of water through the stream exiting the lake will limit the rise in water level of the lake. Therefore, changes in CH_4 production due to increases in rain would be seen first in changes in the active layer before changes in newly flooded lake areas.

The other climatic change of an increase in temperature must also be considered. An increase in temperature that thaws permafrost surrounding Toolik Lake would likely initiate the same changes as increased precipitation. Thawing permafrost would again increase the thickness of the active layer, creating space for a thicker saturated zone around Toolik Lake, while also contributing more water to the active layer. Active layer thaw depths are very sensitive to increases in air temperatures [*Hinkel and Nelson*, 2003] and increases in active layer depth of up to 0.81 cm yr^{-1} have been observed in some Arctic regions [*Oelke et al*., 2004]. On the Alaskan North Slope, *Osterkamp* [2005, 2007] observed permafrost temperature increases of 1 to 4°C over the last few decades. Thawing of permafrost would have the additional methanogenesis-inducing factor of releasing more organic carbon into the saturated zone therein fueling even more methanogenesis.

Aside from increases in active layer depth and saturated zone thickness leading to more CH_4 production in permafrost regions, these increases are predicted to cause an overall shift in the Arctic tundra from a surface water-dominated system to a groundwater-dominated system [*Frey and McClelland*, 2009]. With this shift, we

21698961, 2017, 4, Downloaded from https://agupubs.onlinelibrary.wiley.com/doi/10.1002/2016JG003491 by National Central University, Wiley Online Library on [23/02/2023]. See the Terms and Conditions (https://onlinelibrary.wiley.com/terms-and-conditions) on Wiley Online Library for rules of use; OA articles are governed by the applicable Creative Commons License

expect groundwater flow to become an increasingly important conduit of CH_4 from the active layer to surface water bodies such as lakes and rivers. Already in the Kuparuk River near Toolik Lake, increases in nitrate concentration have been identified as a result of warming permafrost in the region, with nitrate most likely transported to the river by groundwater [*McClelland et al*., 2007; *Osterkamp and Romanovsky*, 1999; *Stieglitz*, 2003]. We expect a similar increase in transport to be true of CH_4 if not already occurring then in the future. Limitations of groundwater transport through the deepening active layer will be in the form of low hydraulic conductivity peat and clay, acting as barriers to flow. More study is needed to make predictions of how much CH_4 transport through the active layer will increase with increasing Arctic temperatures and active layer deepening. An increase in temperatures would also lead to an increased flux of CH_4 from the thaw bulb to the lake, as warmer temperatures support increased methanogenesis.

In conclusion, all of the data we report here indicate that the CH_4 flux to Toolik Lake is at least partially governed by the hydrologic cycle, and changes in that cycle, such as an increase or decrease in precipitation, will have major impacts on the production of CH_4 in the active layer and transport to receiving water bodies. An increase in methanogenesis in the active layer around Toolik Lake would lead to higher flux from the surrounding land into the lake and higher lake water to air fluxes of CH_4, as the areas of highest groundwater influence in the lake coincide with shallow areas around the lake perimeter. This is also where the shorter distance to the water surface will decrease the time during which CH_4 oxidation could occur and lead to a higher water to air CH_4 flux. While our data are from one lake and do not allow global extrapolation, it is not unreasonable to assume that other areas of the tundra would be subject to similar processes and experience similar effects of changes in the hydrologic cycle.

Acknowledgments

This project was funded by NSF-OPP grant ARC 1114485 to A.P. Technical support was provided by the Toolik Lake Long Term Ecological Research Station staff. We would also like to thank Sally McIntyre for her guidance and allowing us to borrow some of her equipment at Toolik Lake and Joseph Murray for collecting samples in 2013. We also thank Carol Kendall and Rachel Mixon at the USGS in Menlo Park for assistance with running the DIC samples. Data from this paper are available in the BCO-DMO database.

References

Anderson, L., J. Birks, J. Rover, and N. Guldager (2013), Controls on recent Alaskan lake changes identified from water isotopes and remote sensing, *Geophys. Res. Lett.*, *40*, 3413–3418, doi:10.1002/grl.50672.

Anisimov, O. (2007), Potential feedback of thawing permafrost to the global climate system through methane emission, *Environ. Res. Lett.*, *2*, 45016, doi:10.1088/1748-9326/2/4/045016.

Badr, O., S. D. Probert, and P. W. O'Callaghan (1991), Atmospheric methane: Its contribution to global warming, *Appl. Energy*, *40*, 273–313.

Blake, L. I., A. Tveit, L. Overeas, I. M. Head, and N. D. Gray (2015), Response of methanogens in Arctic sediments to temperature and methanogenic substrate availability, *PLoS One*, *10*, e0129733, doi:10.1371/journal.pone.0129733.

Boudreau, B. P. (1997), *Diagenetic Models and Their Implementation: Modelling Transport and Reactions in Aquatic Sediments*, Springer, New York.

Brosius, L. S., K. M. Walter Anthony, G. Grosse, J. P. Chanton, L. M. Farquharson, P. P. Overduin, and H. Meyer (2012), Using the deuterium isotope composition of permafrost meltwater to constrain thermokarst lake contributions to atmospheric CH_4 during the last deglaciation, *J. Geophys. Res.*, *117*, G01022, doi:10.1029/2011JG001810.

Brune, A., P. Frenzel, and H. Cypionka (2000), Life at the oxic-anoxic interface: Microbial activities and adaptations, *FEMS Microbiol. Rev.*, *24*, 691–710, doi:10.1016/S0168-6445(00)00054-1.

Bugna, G. C., J. P. Chanton, J. E. Cable, W. C. Burnett, and P. H. Cable (1996), The importance of groundwater discharge to the methane budgets of nearshore and continental shelf waters of the northeastern Gulf of Mexico, *Geochim. Cosmochim. Acta*, *60*, 4735–4746.

Chanton, J. P. (2005), The effect of gas transport on the isotope signature of methane in wetlands, *Org. Geochem.*, doi:10.1016/j.orggeochem.2004.10.007.

Chanton, J., Chaser, L., Glasser, P., and Siegel, D. (2005). Carbon and hydrogen isotopic effects in microbial, methane from terrestrial environments, in *Stable Isotopes and Biosphere—Atmosphere Interactions*, pp. 85–105, Elsevier Academic Press, San Diego, Calif., doi:10.1016/B978-012088447-6/50006-4.

Coleman, D. D., J. B. Risatti, and M. Schoell (1981), Fractionation of carbon and hydrogen isotopes by methane-oxidizing bacteria, *Geochim. Cosmochim. Acta*, *45*, 1033–1037, doi:10.1016/0016-7037(81)90129-0.

Comeau, A. M., T. Harding, P. E. Galand, W. F. Vincent, and C. Lovejoy (2012), Vertical distribution of microbial communities in a perennially stratified Arctic lake with saline, anoxic bottom waters, *Sci. Rep.*, doi:10.1038/srep00604.

Cornwell, J. C., and G. W. Kipphut (1992), Biogeochemistry of manganese- and iron-rich sediments in Toolik Lake, Alaska, *Hydrobiologia*, *240*, 45–59, doi:10.1007/BF00013451.

Dimova, N. T., A. Paytan, J. D. Kessler, K. J. Sparrow, F. Garcia-Tigreros Kodovska, A. L. Lecher, J. Murray, and S. M. Tulaczyk (2015), Current magnitude and mechanisms of groundwater discharge in the Arctic: Case study from Alaska, *Environ. Sci. Technol.*, *49*, 12,036–12,043, doi:10.1021/acs.est.5b02215.

Dlugokencky, E. J., et al. (2009), Observational constraints on recent increases in the atmospheric CH_4 burden, *Geophys. Res. Lett.*, *36*, L18803, doi:10.1029/2009GL039780.

Fisher, R., D. Lowry, O. Wilkin, S. Sriskantharajah, and E. G. Nisbet (2006), High-precision, automated stable isotope analysis of atmospheric methane and carbon dioxide using continuous-flow isotope-ratio mass spectrometry, *Rapid Commun. Mass Spectrom.*, *20*, 200–208, doi:10.1002/rcm.2300.

Frey, K. E., and J. W. McClelland (2009), Impacts of permafrost degradation on Arctic river biogeochemistry, *Hydrol. Processes*, doi:10.1002/hyp.7196.

Garcia-Tigreros Kodovska, F., K. J. Sparrow, S. A. Yvon-Lewis, A. Paytan, N. T. Dimova, A. Lecher, and J. D. Kessler (2016), Dissolved methane and carbon dioxide fluxes in Subarctic and Arctic regions: Assessing measurement techniques and spatial gradients, *Earth Planet. Sci. Lett.*, *436*, 43–55, doi:10.1016/j.epsl.2015.12.002.

Gat, J. R. (1996), Oxygen and hydrogen isotopes in the hydrologic cycle, *Annu. Rev. Earth Planet. Sci.*, *24*, 225–262, doi:10.1146/annurev.earth.24.1.225.

Gibson, J. J., T. W. D. Edwards, and G. G. Bursey (1993), Estimating evaporation using stable isotopes: Quantitative results and sensitivity analysis for two catchments in northern Canada, *Nord. Hydrol.*, *24*, 79–94, doi:10.2166/nh.1993.006.

Happell, J., J. P. Chanton, and W. J. Showers (1994), The influence of methane oxidation on the stable isotopic composition of methane emitted from Florida swamp forests, *Geochim. Cosmochim. Acta*, *58*, 4377–4388, doi:10.1016/0016-7037(94)90341-7.

Hinkel, K. M., and F. E. Nelson (2003), Spatial and temporal patterns of active layer thickness at Circumpolar Active Layer Monitoring (CALM) sites in northern Alaska, 1995–2000, *J. Geophys. Res.*, *108*(D2), 8168, doi:10.1029/2001JD000927.

King, G. M. (1992), Ecological aspects of methane oxidation, a key determinant of global methane dynamics, *Adv. Microb. Ecol.*, *12*, 431–468.

Kling, G. W., W. J. O'Brien, M. C. Miller, and A. E. Hershey (1992), The biogeochemistry and zoogeography of lakes and rivers in Arctic Alaska, *Hydrobiologia*, *240*, 1–14, doi:10.1007/BF00013447.

Lecher, A. L., J. Kessler, K. Sparrow, F. Garcia-Tigreros Kodovska, N. Dimova, J. Murray, S. Tulaczyk, and A. Paytan (2015), Methane transport through submarine groundwater discharge to the North Pacific and Arctic Ocean at two Alaskan sites, *Limnol. Oceanogr.*, *61*, S344–S355, doi:10.1002/lno.10118.

Lecher, A. L., A. T. Fisher, and A. Paytan (2016), Submarine groundwater discharge in northern Monterey Bay, California: Evaluation by mixing and mass balance models, *Mar. Chem.*, *179*, 44–55, doi:10.1016/j.marchem.2016.01.001.

Magen, C., L. L. Lapham, J. W. Pohlman, K. Marshall, S. Bosman, M. Casso, and J. P. Chanton (2014), A simple headspace equilibration method for measuring dissolved methane, *Limnol. Oceanogr. Methods*, *12*, 637–350, doi:10.4319/lom.2014.12.637.

McClelland, J. W., M. Stieglitz, F. Pan, R. M. Holmes, and B. J. Peterson (2007), Recent changes in nitrate and dissolved organic carbon export from the upper Kuparuk River, North Slope, Alaska, *J. Geophys. Res.*, *112*, G04S60, doi:10.1029/2006JG000371.

Oelke, C., T. Zhang, and M. C. Serreze (2004), Modeling evidence for recent warming of the Arctic soil thermal regime, *Geophys. Res. Lett.*, *31*, L07208, doi:10.1029/2003GL019300.

Osterkamp, T. E. (2005), The recent warming of permafrost in Alaska, *Global Planet. Change*, *49*, 187–202.

Osterkamp, T. E. (2007), Characteristics of the recent warming of permafrost in Alaska, *J. Geophys. Res.*, *112*, F02S02, doi:10.1029/2006JF000578.

Osterkamp, T. E., and V. E. Romanovsky (1999), Evidence for warming and thawing of discontinuous permafrost in Alaska, *Permafrost Periglacial Process.*, *10*, 17–37.

Pawlowicz, R., S. A. Baldwin, A. Muttray, J. Schmidtova, B. Laval, and G. Lamont (2007), Physical, chemical, and microbial regimes in an anoxic fjord (Nitinat Lake), *Limnol. Oceanogr.*, doi:10.4319/lo.2007.52.3.1002.

Payette, S., A. Delwaide, M. Caccianiga, and M. Beauchemin (2004), Accelerated thawing of subarctic peatland permafrost over the last 50 years, *Geophys. Res. Lett.*, *31*, L18208, doi:10.1029/2004GL020358.

Paytan, A., A. L. Lecher, N. Dimova, K. J. Sparrow, F. G.-T. Kodovska, J. Murray, S. Tulaczyk, and J. D. Kessler (2015), Methane transport from the active layer to lakes in the Arctic using Toolik Lake, Alaska, as a case study, *Proc. Natl. Acad. Sci. U.S.A.*, *112*(12), 3636–3640, doi:10.1073/pnas.1417392112.

Powelson, D. K., J. P. Chanton, and T. Abichou (2007), Methane oxidation in biofilters measured by mass-balance and stable isotope methods, *Environ. Sci. Technol.*, *41*, 620–625, doi:10.1021/es061656g.

Reeburgh, W. S. (2013), Global methane biogeochemistry, in *Treatise on Geochemistry*, 2nd ed., pp. 71–94, Elsevier, doi:10.1016/B978-0-08-095975-7.00403-4.

Segarra, K. E. A., C. Comerford, J. Slaughter, and S. B. Joye (2013), Impact of electron acceptor availability on the anaerobic oxidation of methane in coastal freshwater and brackish wetland sediments, *Geochim. Cosmochim. Acta*, *115*, 15–30, doi:10.1016/j.gca.2013.03.029.

Smith, L. C., Y. Sheng, G. M. MacDonald, and L. D. Hinzman (2005), Disappearing Arctic lakes, *Science*, *308*, 1429, doi:10.1126/science.1108142.

Stafford, J. M., G. Wendler, and J. Curtis (2000), Temperature and precipitation of Alaska: 50 year trend analysis, *Theor. Appl. Climatol.*, *67*, 33–44, doi:10.1007/s007040070014.

Stieglitz, M. (2003). The role of snow cover in the warming of arctic permafrost. *Geophys. Res. Lett.*, *30*(13), 1721, doi:10.1029/2003GL017337.

Waldron, S., J. M. Lansdown, E. M. Scott, A. E. Fallick, and A. J. Hall (1999), The global influence of the hydrogen isotope composition of water on that of bacteriogenic methane from shallow freshwater environments, *Geochim. Cosmochim. Acta*, *63*, 2237–2245, doi:10.1016/S0016-7037(99)00192-1.

Walker, D. A., and A. W. Balser (2004), *Surficial Geology of the Upper Kuparuk River Region*, Fairbanks, Alaska.

Walter, K. M., L. C. Smith, and F. S. Chapin (2007), Methane bubbling from northern lakes: Present and future contributions to the global methane budget, *Philos. Trans. R. Soc., A*, *365*, 1657–76, doi:10.1098/rsta.2007.2036.

Walter, K. M., J. P. Chanton, F. S. Chapin, E. A. G. Schuur, and S. A. Zimov (2008a), Methane production and bubble emissions from arctic lakes: Isotopic implications for source pathways and ages, *J. Geophys. Res.*, *113*, G00A08, doi:10.1029/2007JG000569.

Walter, K. M., M. Engram, C. R. Duguay, M. O. Jeffries, and F. S. Chapin (2008b), The potential use of synthetic aperture radar for estimating methane ebullition from Arctic lakes, *J. Am. Water Resour. Assoc.*, *44*, 305–315, doi:10.1111/j.1752-1688.2007.00163.x.

Whalen, S. C., and J. C. Cornwell (1985), Nitrogen, phosphorus, and organic carbon cycling in an Arctic lake, *Can. J. Fish. Aquat. Sci.*, *42*, 797–808, doi:10.1139/f85-102.

Whiticar, M. J. (1999), Carbon and hydrogen isotope systematics of bacterial formation and oxidation of methane, *Chem. Geol.*, *161*, 291–314, doi:10.1016/S0009-2541(99)00092-3.

Whiticar, M., E. Faber, and M. Schoell (1986), Biogenic methane formation in marine and freshwater environments: CO_2 reduction vs. acetate fermentation—Isotope evidence, *Geochim. Cosmochim. Acta*, *50*(5), 693–709, doi:10.1016/0016-7037(86)90346-7.

Yamamoto, S., J. B. Alcauskas, and T. E. Crozier (1976), Solubility of methane in distilled water and seawater, *J. Chem. Eng. Data*, *21*, 78–80, doi:10.1021/JE60068a029.

Yarnes, C. (2013), Delta13C and Delta2H measurement of methane from ecological and geological sources by gas chromatography/combustion/pyrolysis isotope-ratio mass spectrometry, *Rapid Commun. Mass Spectrom.*, *27*, 1036–1044, doi:10.1002/rcm.6549.

Zimov, S., E. Schuur, and F. S. Chapin III (2006), Permafrost and the global carbon budget, *Science*, *312*, 1612–1613.

21698961, 2017, 4, Downloaded from https://agupubs.onlinelibrary.wiley.com/doi/10.1002/2016JG003491 by National Central University, Wiley Online Library on [23/02/2023]. See the Terms and Conditions (https://onlinelibrary.wiley.com/terms-and-conditions) on Wiley Online Library for rules of use; OA articles are governed by the applicable Creative Commons License